Dielectric properties of *Artemia* cysts at low water contents

Evidence for a percolative transition

F. Bruni,* G. Careri,* and J. S. Clegg

*Dipartimento di Fisica, Universita di Roma I, Roma 00185, Italy; University of California, Bodega Marine Laboratory, Bodega Bay, California 94923

ABSTRACT Cellular cysts of the crustacean *Artemia* provide a useful model for studies on water-dependent mechanisms in cellular function because they can undergo reversible cycles of dehydration-rehydration. We explored their dielectric behavior over the frequency range of 10 kHz to 1 MHz, at water contents between near zero and 0.5 g H_2O/g dry weight (g/g). The dc conductivity and static dielectric permittivity were evaluated from electrostatic analysis of data obtained with a three-layered capacitor. Below cyst hydrations of 0.05 g/g, negligible dielectric response was observed at all frequencies. Between 0.05 and 0.25 g/g the permittivity increased sharply then reached a near plateau up to cyst hydrations close to 0.35 g/g, above which a second abrupt increase occurred. Values for the dielectric loss (tan δ) exhibited frequency-dependent peaks over the hydration range of 0.05–0.3 g/g, followed by an abrupt increase near 0.35 g/g, an hydration at which metabolism is first initiated in this system. These hydration-dependent dielectric changes are compared with previous studies on the biology and physics of this system, and evaluated by a model involving percolative ionic (likely protonic) conduction. Percolative behavior is characterized by a sharp increase in conductivity at a critical threshold of hydration (h_c) according to a power law in which the exponent, t, equals 1.65 for a three-dimensional infinite lattice. For the *Artemia* cyst, $t = 1.64$ above $h_c = 0.35$ g/g, which is in excellent agreement with theory. These results are compared to similar studies on lysozyme which also exhibits percolative behavior connected with the onset of biological function.

INTRODUCTION

Percolation theory (1) has been shown to apply to a broad range of chemical and physical phenomena where spatially random processes and topological disorder are of importance. The central issue at the heart of the percolation model is the presence of a percolative transition where long-range connectivity between the elements of a system suddenly appears. Behavior near the threshold can be described by a set of critical exponents, analogous to those used to describe phase transitions of other kinds. An example of a typical percolative process is electrical conduction through a mixture of conducting and nonconducting elements, a system that displays a transition and a specific power law dependence of the conductivity at the critical threshold value on the concentration of conducting elements. Diffusion on a randomly filled lattice is also a percolative process, and it can be shown to be formally equivalent to conduction (1). Previous work has shown that hydrated lysozyme powders exhibit dielectric behavior owing to proton conductivity that is in good agreement with the predictions of percolation theory (2, 3). In that case the conductivity reflects the motion of protons along threads of hydrogen-bonded water molecules on or very near the surface of the protein; however, long-range proton displacement appears only above the critical hydration for percolation. A similar experimental approach has been taken using the purple membrane of *Halobacterium halobium* and the results (unpublished) can also be explained by the percolation model: the hydration dependence of the protonic conductivity is characteristic of a two-dimensional percolative system.

To evaluate the possible participation of percolative transitions in more complex biological systems, we have studied the dielectric behavior of the cysts of *Artemia* at low water contents. This system is ideal for such work because of its natural ability to undergo repeated, reversible cycles of dehydration and rehydration and because its physical properties and biochemistry have been studied extensively by a number of techniques (4–7). In this paper we will describe the hydration dependence of the DC conductivity and static dielectric permittivity. Furthermore, we will show that, above a critical hydration threshold, this behavior is fully consistent with a three-dimensional percolation model in which subregions of fixed geometry could be imbedded within randomly filled regions of the system in which clustering can be accommodated. The stochastically arranged conducting elements can be any groups bearing labile hydrogens, includ-

Dr. Bruni's present address is Department of Plant Biology, Cornell University, Ithaca, NY 14853.

Address correspondence to Dr. Clegg, P.O. Box 247, Bodega Bay, CA 94923.

0006-3495/89/02/331/08 $2.00

ing those of water molecules. The critical hydration threshold for the percolative transition is found to be very close to that required for the initiation of metabolic activity in this system.

MATERIALS AND METHODS

Experimental apparatus

The measurement apparatus consisted of a capacitor assembly mounted on a balance enclosed in a vapor-tight box. Previous papers (2, 8) have described details of the apparatus, and the measurement of dielectric properties at frequencies from 10 kHz to 10 MHz, for hydration levels from wet powders to the lowest hydration limit where the evaporation rate is zero. The apparatus was designed to monitor simultaneously changing evaporation rates and dielectric properties. To avoid artifacts induced by electrodes, we put our samples (about 1 mm thick) on partly filled glass dishes inside a parallel-plate capacitor, thus eliminating contact with the plates. The electrode diameter was 2.5 cm.

All data were automatically recorded every few minutes on magnetic tape for further study. A typical run lasted about 1 d and more than 300 data points were collected per sample. This provided an essentially continuous record of the dielectric properties as a function of the sample's hydration level (h), which is expressed here as grams of H_2O/gram of dry cyst weight (g/g for brevity). The evaporation rate (E) is immediately evaluated from the weight loss per unit time and is expressed as grams of H_2O/min. We (4) have shown that negligible hysteresis is present in the water sorption characteristics of these cysts over the hydration range under study here, suggesting that we are dealing with a reversible process.

During the measurements the hydration of each sample was varied from the starting condition, which was a wet sample obtained by isopiestic equilibration against pure water (for more details, see Table 1), to the final limiting low hydration, h_0. The hydration level was calculated for each time point from the weight at that time of the partially hydrated sample and from the weight determined at the end of the experiment, after the evaporation rate had reached zero. At that end point, a residual amount of water remains, representing the hydration level h_0. This was determined for each sample by heating at 105°C overnight (5).

The dielectric apparatus gives values for the capacitance and the dielectric loss factor of the composite capacitor containing the sample. To investigate the dielectric behavior of the sample over the entire hydration region, we analyzed the hydration dependence of the capacitance at various frequencies. Using these capacitance data, and dielectric theory for a composite capacitor (9), we evaluated the static permittivity (ϵ), and the DC conductivity (σ) of the sample. From dielectric theory (9), the frequency-dependent capacitance $C_{tot}(f)$ of the three-layer capacitor (air [1], sample [2], glass [3]) at a fixed water content of the sample, can be expressed as:

$$C_{tot}(f) = \frac{\epsilon_0 L}{\Sigma_k d_k}\,\epsilon'_{tot}(f) = \epsilon_0 L\left\{\Sigma_k \frac{\epsilon_k}{d_k}\frac{f^2\tau_k^2}{(f^2\tau_k^2+1)}\right\}^{-1}, \quad (1)$$

where ϵ_0 is the vacuum permittivity, L is the electrode area, d_k is the thickness of the k-layer, $\epsilon'_{tot}(f)$ is the real part of the complex permittivity $\epsilon^*_{tot}(f)$ of the composite capacitor, and τ_k is the relaxation time equal to $\epsilon_0\epsilon_k/\sigma_k$ where ϵ_k and σ_k are respectively the static permittivity and the DC conductivity of the k-layer. By assuming that the dry air and glass layers display static permittivities $\epsilon_1 = 1$ and $\epsilon_3 = 3$, respectively, and neglecting their DC conductivity, the above equation can be written as:

$$C_{tot}(f) = \frac{\epsilon_0 L\epsilon^*}{d_2}\left\{1 + \frac{\epsilon^*}{\epsilon_2}\left(\frac{f^2\tau_2^2}{1+f^2\tau_2^2}\right)\right\}^{-1}, \quad (2)$$

where ϵ^* is a constant equal to $(d_2\epsilon_1\epsilon_3)/(d_1\epsilon_3 + d_3\epsilon_1)$. The only two unknowns in the above equation are ϵ_2 and σ_2 (static permittivity and DC conductivity of the sample) and they can be evaluated by a standard least-squares best-fit procedure.

TABLE 1 Hydration conditions and parameters

Sample number	Time	Temperature*	Humidity (%)	Cyst water content
	h	°C	%	H_2O g dry wt
1	46	4	100	0.49
2	45	25	97	0.54
3	19	4	100	0.38
4	82	25	97	0.95

*± 0.1°C

Artemia cysts

Cysts of the brine shrimp *Artemia* are early embryos covered by a complex chitinous shell, most of which can be chemically removed (4, 5). There are about 4,000 tightly packed, morphologically similar cells per cyst (about 220-μm diam spheres when fully hydrated) with virtually no extracellular space. The cysts have the ability to tolerate essentially complete but fully reversible desiccation, thus providing excellent material for the study of hydration dependent properties. These and other features of this system have been described in considerable detail (4–7). This study used cysts from the solar salt operation near Hayward, CA which were purchased from San Francisco Bay Brand, Newark, CA. The commercial cysts were washed, redried, and stored at −20°C. Preparations of shells, free from embryos, were obtained by previously described methods (5). The viability of the cyst population used in this study was 89% as judged by their ability to produce swimming larvae (nauplii) when incubated for 48 h in seawater at 25°C.

RESULTS

Initial studies assessed the reliability of our technique for this experimental system, and determined a convenient sample weight that would ensure good uniformity of cyst hydration and a high sensitivity of dielectric response. We report data for four dehydration runs, made on different samples of the same material, hydrated (Table 1) and then dehydrated (Table 2) by different procedures. Although all these runs offer a self-consistent and reproducible set of data, run 1 is the best representative for the low hydration range to be considered in this paper (0–0.4 g/g). These data will be analyzed in detail next.

Fig. 1 shows the dehydration kinetics of this sample. Similar plots (not shown) were obtained for the time dependence of the dielectric data at 10 frequencies and for the evaporation rate (E). Instead of reporting the raw

TABLE 2 Dehydration conditions and parameters

Sample number	Time	Temperature	Dry* flux	C_o	Dry weight
	h	°C		*pF*	*g*
1	8	28	Off	3.0575	0.2844
2	8	28	Off	2.3094	0.2630
3	21	28	On	2.9204	0.2802
4	8	28	On	1.7819	0.2791

This value for the capacitance has been measured at 10 kHz, but it should be noted that at the end of the experiments, capacitance values are essentially frequency independent (see Fig. 5).
*Dry air flow over the sample at 100–200 liter/h.

data, we eliminate the time parameter and display in Figs. 2, 3, and 4, respectively, the reduced capacitance (C/C_0, where C_0 is the capacitance at $h = h_0, f = 10$ kHz, as indicated in Table 2), dielectric loss (tan δ) and the evaporation rate (E) as a function of cyst water content: these three plots describe the intrinsic properties of the hydrated sample. Note the transitions observed in all three parameters at h close to 0.35: they will prove to be of importance when we interpret these data later.

Figs. 5 and 6 show the capacitance of cysts as a function of frequency at selected values of cyst hydration. In Fig. 7 a plot of tan δ against frequency is given for the same hydration levels shown in Fig. 6. From the capacitance data at three frequencies (10, 20, and 40 kHz) we evaluated the DC conductivity (Fig. 8) and static dielectric permittivity (Fig. 9) by means of an electrostatic analysis for the three-layer capacitor network (see Materials and Methods).

The only assumption needed for this evaluation is the occurrence of one relaxation time in the frequency range considered. This is essentially true (see Fig. 3 and also Fig. 7) at high hydration, for $h \geq 0.35$, and in the low

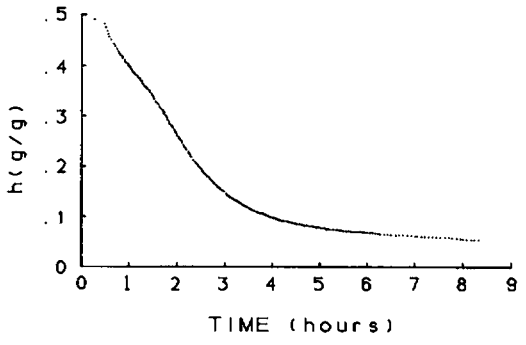

FIGURE 1 Cyst hydration level, h, (grams of H_2O/gram of dry weight) as a function of time (hours) during run 1, indicated in Table 1. Each data point represents one independent measurement.

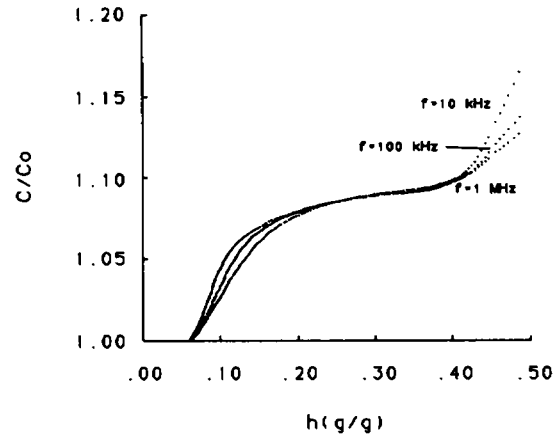

FIGURE 2 Reduced capacitance of cysts, C/C_0, at three different frequencies plotted versus hydration level, h, (g/g) for run 1. C_0 is the dry weight capacity, at $h = h_0$, indicated in Table 1, and is essentially frequency independent.

hydration region for $h \leq 0.20$, but not in the range between $0.20 < h < 0.35$. For this reason the conductivity and the static permittivity data plotted in Figs. 8 and 9 are not reliable in the range $0.20 < h < 0.35$.

Finally, and for reasons to be discussed later, we have measured the reduced capacitance of shells isolated free from intact cysts (Fig. 10). Note the absence of any abrupt increase in C/C_0 as a function of h. Also, it should be pointed out that in intact cysts at $h = 0.35$, the shells only contain a water content of about 0.1 g/g (6, 7), at which hydration they exhibit virtually no permittivity (Fig. 10).

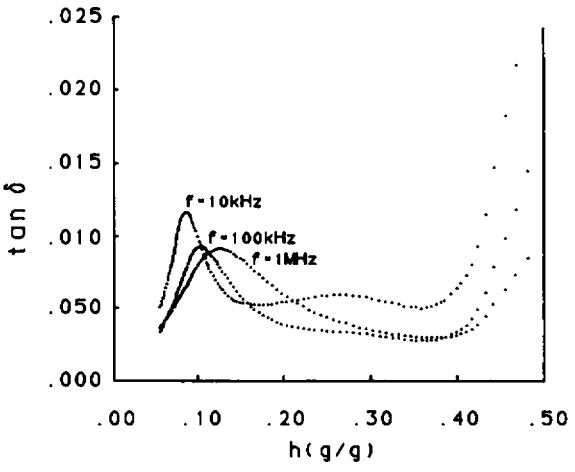

FIGURE 3 The dielectric loss factor, tan δ, as a function of cyst hydration level h (g/g) for run 1, at three different frequencies.

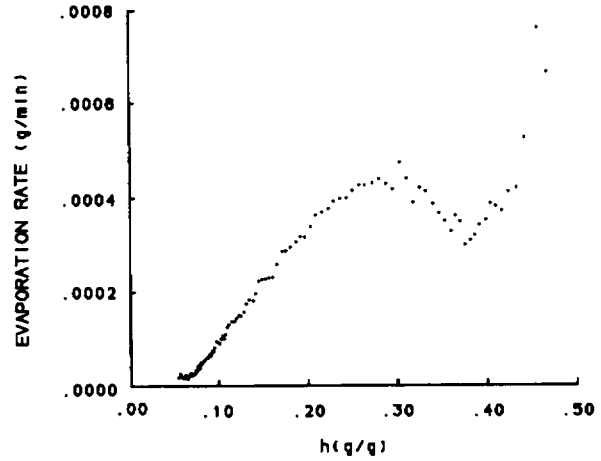

FIGURE 4 Evaporation rate, E, (grams of H_2O/minute) as a function of cyst hydration level h (g/g) for run 1.

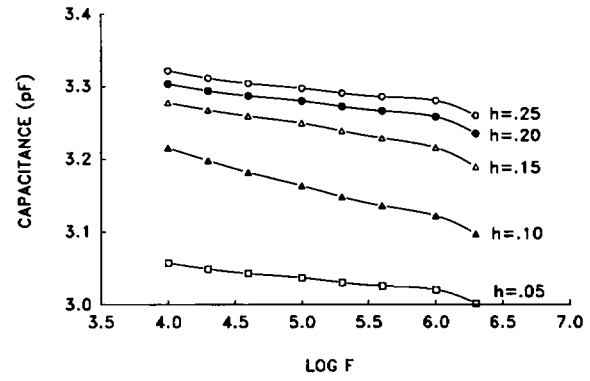

FIGURE 5 Cyst capacitance, C (picofarad) as a function of frequency, f, (Hertz) for run 1 at different hydration levels h (g/g), at nearly constant hydration increment, $h = 0.05$ (g/g).

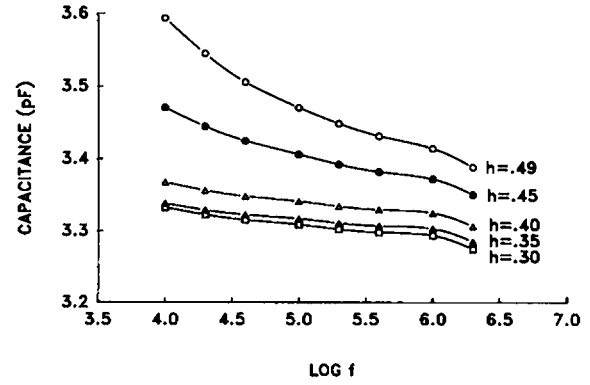

FIGURE 6 The same conditions as Fig. 5, but for higher hydration levels.

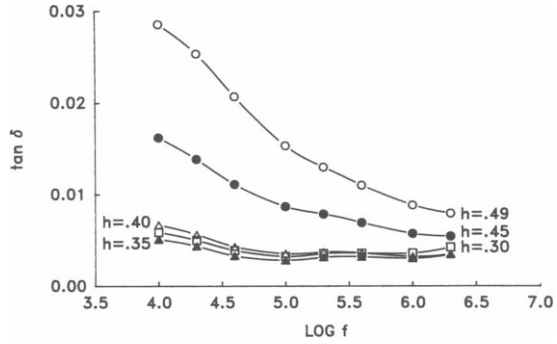

FIGURE 7 The dielectric loss factor, tan δ, as a function of frequency for the same run and the same hydration levels as those of Fig. 6.

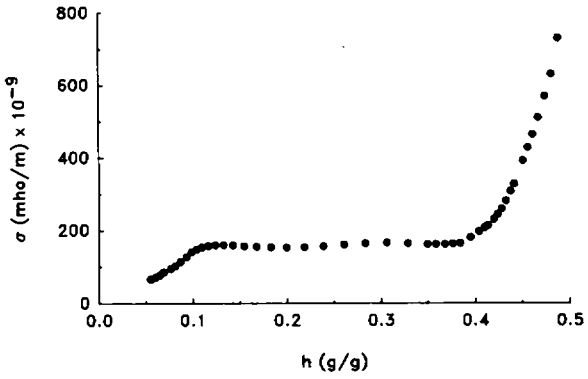

FIGURE 8 The DC conductivity, σ, (Siemens per meter) of the cyst sample used in run 1, plotted vs. hydration level h (g/g).

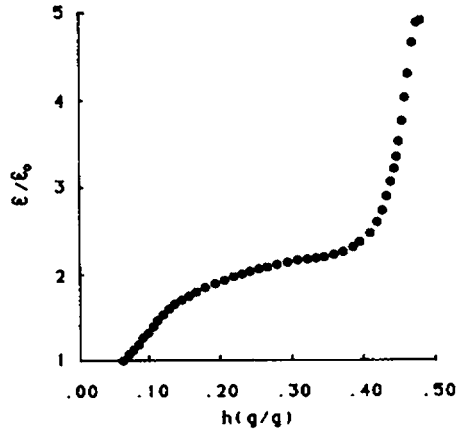

FIGURE 9 The static dielectric reduced permittivity, ϵ/ϵ_0, for the same sample displayed in Fig. 8.

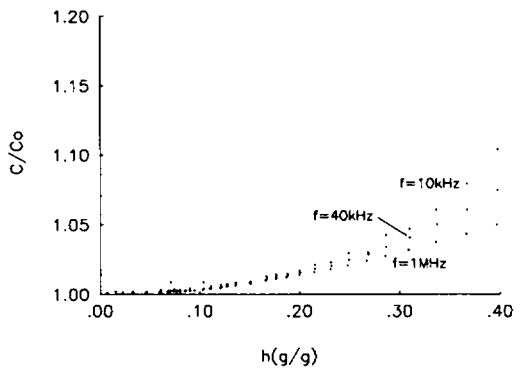

FIGURE 10 Reduced capacitance (C/C_0) of shells as a function of their hydration at three applied frequencies. Because shells contain less water on a g/g basis than do intact cysts equilibrated at the same humidity the values of h are not directly comparable. At a cyst hydration of 0.35 g/g, the shells contain only about 0.1 g/g (6, 7). C_0 = 1.7885 pF, f = 10 kHz.

DISCUSSION

Interpretation of the data presented here will be facilitated by subdividing the cyst hydration span considered in this paper into four ranges as follows, based on previous work (6, 14): (*a*) 0–0.05; (*b*) 0.05–0.1; (*c*) 0.1–0.35; and (*d*) >0.35. Results for each hydration range, *h* (in g/g), will be discussed below, first from a physical point of view and then from a biological one. For convenience we will discuss hydration-dependent events in the direction of increasing hydration since hydration-dependent hysteresis is negligible over this range (5, 11).

Physical interpretation

Range *a*

This region is characterized by a vanishingly small dielectric response and evaporation rate. Within experimental error one may say that all the measured properties do not differ from those of a completely dry sample. In this range of *h* the water molecules must be very tightly bound, and essentially an integral part of the structure (sites) with which they associate. Results from proton nuclear magnetic resonance (NMR), differential scanning calorimetry (DSC), and microwave dielectrics clearly support that interpretation (6, 7).

Range *b*

In this region we propose, on the basis of the data in Figs. 2, 6, and 8 that some charged and mobile water-induced structures are built that, once formed, display well-defined DC conductivity values. The results shown in Fig. 4 indicate that the water in the cysts becomes progressively more mobile as the higher end of this hydration range is reached. We envision that this water is likely to fluctuate in position from site to site. The dielectric loss factor (tan δ) as a function of the hydration level, displays a neat peak (Fig. 3) which is frequently dependent. Such results are typical of the presence of several competing structures that finally merge over a small frequency range and then become hydration-independent towards the upper end of this *h* range. Previous work on water sorption isotherms of *Artemia* cysts (4) reveals a sharp decrease in differential entropy changes ($\Delta\bar{S}$) associated with the sorbed water over h of 0.05–0.1; above *h* of 0.1, $\Delta\bar{S}$ levels off and is close to that of ordinary bulk water. These changes in the property of water at *h* close to 0.1 are also detected by NMR and DSC (6, 7) and density measurements (11). Therefore, we propose that the conductivity behavior shown in Fig. 8 of the present paper can be interpreted in terms of the dissipative contribution of dipoles and charges occurring in the inner structure of the cysts which become mobile and/or polarizable only when in contact with large numbers of water molecules, hydrogen bonded in three dimensions.

Another feature of hydration range *b* is the initiation of an increase in static permittivity (Fig. 9). In addition to contributions from "mobile water," this could reflect water-induced phase transitions associated with the formation of functional biological structures such as membranes. As is well known, biological membranes are characterized by a high and constant value of capacity in the frequency region considered here, and by a definite low value for the DC conductivity (9). Also highly relevant is extensive work (10) showing that membranes undergo extensive water-induced phase transitions at hydrations in the vicinity of 0.2 g/g, and that these transitions are modified by sugars such as trehalose, a major component of *Artemia* cysts, events which are critical to membrane stabilization. A quantitative evaluation of the observed permittivity increase in terms of membrane formation or alteration is difficult and probably impossible because of the uneven distribution of these membranes in the electric field of our capacitor. However, it is worth pointing out that a water-induced change of membrane thickness has been observed in soybean preparations at precisely the same water content region (0.05–0.1 g/g) by Seewaldt et al. (12). We have also observed marked changes in the density (11) and partial heat capacity (7) of cyst water as this hydration region is traversed.

Range *c*

This region is characterized by a flat plateau in the conductivity (Fig. 8) and by a steady increase of the permittivity towards a limiting value at the upper end of this hydration region (Figs. 1 and 9). As already men-

tioned above, the occurrence of more than one relaxation time in this hydration range makes the evaluation of these quantities less reliable. Nevertheless, this permittivity increase might also reflect the process of functional membrane formation which, we propose, is fully accomplished in this region because of the increase in hydration, while the dissipative relaxation processes postulated to first occur in the lower part of hydration range *b* remain as an essentially constant contribution.

Range *d*

Above h of about 0.35 all dielectric and evaporation rate data display a strong increase with increasing hydration (Figs. 2–4, 6–9). Since the DC conductivity (Fig. 8) shows this most clearly, we shall discuss it in detail.

We pursue the possibility that these changes in the DC conductivity above $h = 0.35$ can be described by the percolative model which has already been applied to lysozyme powders (2, 3). In the present case we suggest that, in addition to the low constant DC conductivity, a new ionic conduction process is initiated abruptly near the critical threshold, $h_c = 0.35$.

The completely dry cyst is dielectrically frozen (6, 7) and it seems reasonable to suppose that virtually all intracyst structures are in very close contact and certainly cannot be separated by a bulk aqueous phase. As more and more water enters these cysts we postulate that a point is reached (h_c) at which percolative ionic conduction begins. Percolative behavior is characterized by a sharp increase in the conductivity (σ) near and above h_c, according to a power law (1)

$$\sigma - \sigma_c \propto (h - h_c)^t \qquad (3)$$

where $t = 1.65$ for a three-dimensional infinite lattice, and σ_c is the conductivity at h_c. We have evaluated the validity of Eq. 1 and the results are displayed in Fig. 11. A value for t of $1.64 \pm <0.01$ is obtained, in good agreement with theoretical prediction. We hasten to recognize that other interpretations are possible, and that other mechanisms could be involved here; nevertheless, this agreement is certainly encouraging.

We admit that we cannot determine with certainty the nature of the ions giving rise to the percolative conduction process above h_c from the present data. In the cases of lysozyme powders (2, 3) studied by the same technique in the same frequency range, these ions were proven to be protons because of the isotopic effect measured in H_2O and D_2O studies; moreover, the same isotopic effect has also been detected in wheat seeds as reported in previous work (13). We have been unable to carry out a similar check using D_2O in *Artemia* cysts because D_2O affected their hydration in a more complex way and the conductivity data could not be compared with H_2O hydrated cysts

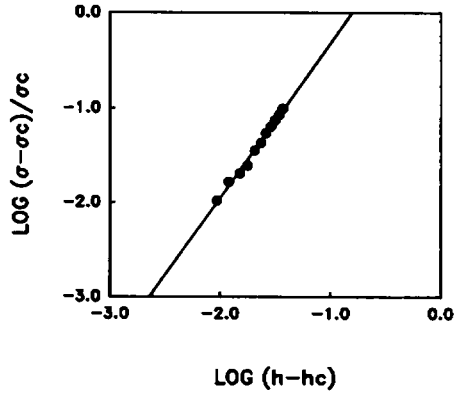

FIGURE 11 The reduced conductivity increment above h_c plotted against the hydration increment, h-h_c, to fit the data of region (*c*) by Eq. 1 (text). σ_c is the conductivity at h_c from the data of Fig. 8. The straight line is the best-fitted power law with an exponent $t = 1.635$, and a variance 0.001, assuming $h_c = 0.35$ (g/g), $\sigma_c = 161.060$ (S/m) $\times 10^{-9}$.

in terms of a kinetic factor $\sqrt{2}$. Until further analysis of this sort is carried out on *Artemia* cysts to evaluate other ion contributions we can only propose tentatively that above the critical hydration level a three-dimensional thread of water molecules becomes distributed within the internal structure of the cysts which allows for ionic (likely protonic) displacement along this thread over distances considerably longer than single ion size. This same critical hydration level for percolative ionic conductivity also coincides with the onset of metabolism in these cysts which will be considered later in this paper.

We should point out that the value of the threshold h_c in different runs is somewhat variable. We have shown in the case of run 1 that the threshold is clearly 0.35, and we consider this our best case. In the other three cases we have verified that, for each run, a particular h_c value exists where all the dielectric properties and the evaporation rate displayed quite the same behavior as run 1 at $h_c = 0.35$. However, the h_c value of each run does vary, and was found to depend strongly upon the maximum hydration level (h_{max}) reached in the incubator before dehydration was begun:

Sample	h_{max}	h_c
1	0.49	0.35
2	0.54	0.45
3	0.38	0.26
4	0.95	0.65

The anomalous value for $h_{max} = 0.95$ is probably due to the fact that when cyst hydrations exceed 0.65 g/g the cells become very active metabolically and this has profound effects on cyst properties (4–7): the cells metaboli-

cally manipulate their own hydration levels under these circumstances. On the other hand, samples 2 and 3 displayed a critical exponent $t = 1.65$, in good agreement with the value of sample 1 (see Fig. 12).

Before ending this section, we recognize that a different and more trivial explanation for the strong increase of dielectric parameters in this region could be offered in terms of the possible capillary condensation occurring at the contacts between cysts. This phenomenon is well known and we considered that this might be involved at the higher hydration region. We believe this is not the case, because a sample consisting of shells should have displayed an even more intense capillary condensation, but that was not observed: the reduced capacity of shells (reported in Fig. 10) did not show any abrupt increase at hydrations of the type found for the cyst samples (see Fig. 2).

Biological interpretation

As mentioned above, the hydration dependence of cyst metabolism has been mapped in considerable detail in this system (6, 14, 15). With regard to the hydration range of interest in this paper (0–0.40 g/g) it is noteworthy that detectable metabolic activity is not initiated until the cysts reach a water content very near 0.35 g/g, precisely the value of h_c, which, we propose, initiates percolation events. We have emphasized the potential involvement of membrane hydration in the proposed onset of percolative ionic conductivity at that hydration, and consider that possibility to be of potential importance in the initiation of metabolism in the cells of these cysts. But other possibilities also should be mentioned here.

It now seems very likely that most of the enzymes of intermediary metabolism are organized into complexes, probably associated with the cytoplasmic matrix, and are

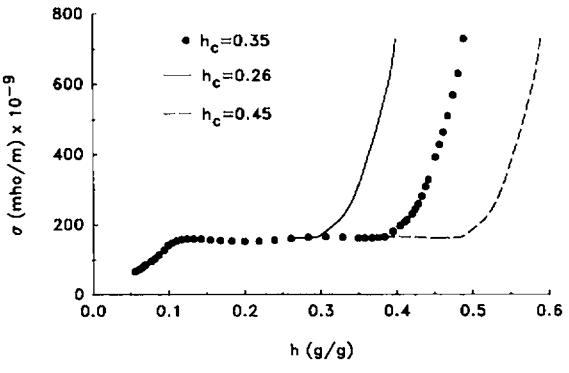

FIGURE 12 The DC conductivity, σ (S/m), of the cyst samples used in runs 1 (h_c = 0.35 g/g), 2 (h_c = 0.45), and 3 (h_c = 0.26), plotted vs. hydration level h (g/g).

not randomly dispersed within the aqueous phases of cells. The evidence for that contention is now abundant and the subject of several recent books and reviews (15–18), including the specific case of *Artemia* cysts (14). One can easily envision the possibility that the initiation of intermediary metabolism and the postulated percolative transition may be intimately related. Thus, it may be proposed on these grounds that the establishment of random space connectivity of ionic pathways may facilitate formation and/or function of enzyme–enzyme and/or enzyme–cytomatrix associations. The striking coincidence of the onset of metabolic activity observed at 0.35 g/g with the proposed initiation of percolative ionic conductivity certainly suggests a possible mutual dependence of both of these hydration-dependent processes. These correlations must, of course, be subjected to further experimental test in order to establish their general validity and potential causal connection.

Finally, we point out that the dielectric properties of *Artemia* cysts have been described up to frequencies of 70 GHz and over their entire hydration range (19, 20).

We thank Victoria Milam and Diane Cosgrove for skillful manuscript preparation.

This study was supported in part by grant DCB-8820347 from the National Science Foundation to Dr. Clegg, and in part by Gruppo Nazionale Struttura della Materia to Dr. Careri.

Received for publication 11 July 1988 and in final form 17 October 1988.

REFERENCES

1. Zallen R. 1983. The Physics of Amorphous Solids. John Wiley & Sons, New York.
2. Careri, G., A. Giansanti, and J. A. Rupley. 1986. Proton percolation on hydrated lysozyme powders. *Proc. Natl. Acad. Sci. USA.* 83:6810–6814.
3. Careri, G., A. Giansanti, and J. A. Rupley. 1988. Critical exponents of protonic percolation in hydrated lysozyne powders. *Phys. Rev. A* 37:2703–2705.
4. Clegg, J. S. 1978. Interrelationships between water and cell metabolism in *Artemia* cysts. VIII. Sorption isotherms and derived thermodynamic quantities. *J. Cell. Physiol.* 94:123–138.
5. Clegg, J. S. 1986. *Artemia* cysts as a model for the study of water in biological systems. *Methods Enzymol.* 127:230–236.
6. Clegg, J. S. 1986. The physical properties and metabolic status of *Artemia* cysts at low water contents. *In* Membranes, Metabolism and Dry Organisms. C. Leopold, editor. Cornell University Press, New York. 169–187.
7. Clegg, J. S. 1987. On the physical properties and roles of intracellular water. *In* The Organization of Cell Metabolism. G. R. Welch and J. S. Clegg, editors. Plenum Press, New York. 41–56.

8. Careri, G., and A. Giansanti. 1986. Dielectric properties of nearly dry biological systems at megaherz frequencies. *In* Membranes, Metabolism and Dry Organisms. C. Leopold, editor. Cornell University Press, New York. 273–285.

9. Pethig, R. 1979. Dielectric and Electronic Properties of Biological Materials. John Wiley & Sons, New York. 412 pp.

10. Crowe, J. H., and L. M. Crowe. 1986. Stabilization of membranes in anhydrobiotic organisms. *In* Membranes, Metabolism and Dry Organisms. C. Leopold, editor. Cornell University Press, New York. 188–209.

11. Clegg, J. S. 1984. Interrelationships between water and cellular metabolism in *Artemia* cysts. XI. Density measurements. *Cell Biophys.* 6:153–161.

12. Seewaldt, V., D. A. Priestley, A. C. Leopold, G. W. Feigenson, and F. Goodsaid-Zaldvondo. 1981. Membrane organization of soybean seeds during hydration. *Planta.* 152:19–23.

13. Careri, G., and A. Giansanti. 1984. Deuterium effect in the dielectric losses of wheat seeds. *Lett. Nuovo Cimento.* 40:193–196.

14. Clegg, J. S. 1981. Interrelationships between water and cellular metabolism in *Artemia* cysts. IX. Evidence for the organization of "soluble" enzymes. *Cold Spring Harbor Symp. Quant. Biol.* 46:23–37.

15. Clegg, J. S. 1984. Properties and metabolism of the aqueous cytoplasm and its boundaries. *Am. J. Physiol.* 246:R133–151.

16. Bhargava, P. M. 1985. Is the soluble phase of cells structured? *BioSystems.* 18:135–139.

17. Srere, P. A. 1987. Complexes of sequential metabolic enzymes. *Annu. Rev. Biochem.* 56:21–56.

18. Welch, G. R., and J. S. Clegg. 1987. The Organization of Cell Metabolism. Plenum Press, New York. 1–389.

19. Clegg, J. S., S. Szwarnowski, V. E. R. McClean, R. J. Sheppard, and E. H. Grant. 1982. Interrelationships between water and cell metabolism in *Artemia* cysts. X. Microwave dielectric studies. *Biochim. Biophys. Acta.* 721:458–468.

20. Clegg, J. S., V. E. R. McClean, S. Szwarnowski, and R. J. Sheppard. 1984. Microwave dielectric measurements (0.8–70 GHz) on *Artemia* cysts at variable water content. *Phys. Med. Biol.* 29:1409–1419.